Research Article

Study of Structural and Dielectric Properties of Gold Embedded ZnO Nanohairs Fabricated by Thermal Oxidation Methods

S. Srivastava

Material Science & Metallurgical Engineering, Maulana Azad National Institute of Technology, Bhopal M.P. (India)

Abstract

Zinc oxide nano hair/needle was synthesized from the thermal oxidation of zinc metal at temperature range from 300-700°C for 2hrs by controlling the oxygen partial pressure, the beautiful results give optimum information about the formation of ZnO nanostructures at the surface of metallic Zinc. In initial stage the developed structure was again modified by sequential and step wise heating of Zn-metal in open atmosphere. Each and every times, the thickness of the oxide becomes increase. This growth was catalyzed by the presence of the gold in the matrix. The morphology of the grown structure was investigated by SEM observation. Subsequent heating of the sample in open atmosphere, the sizes of growing needle of ZnO nanostructure becomes drastic change and elongated in those directions, where the heat transfer effect is nullified. At the higher temperature, the chance of oxidation is to be increase, because of higher rate constant of the nucleation. At this level, oxygen partial pressure plays very crucial role in nucleation of ZnO needle structure. The beautiful needle of ZnO with well separated from each other was obtained. This was identified by XRD and Raman investigation. At the higher temperature, the dielectric of the nanostructure are reported and also varied with annealing temperature.

***Correspondence**
S. Srivastava
Email: s.srivastava.mmsme@gmail.com
Mobile number: +919479910003

Keywords: Thermal oxidation, Annealing, Nanohair/ Nanoneedle, Raman Spectroscopy.

Introduction

Zinc oxide, ZnO is a versatile semiconducting material with direct band gap (3.37 eV) and has high exciton binding energy (60 meV) has a great attention from silent feature in device fabrication such as light emitting diode, solar cells and various type of sensors [1-2]. ZnO as a Microwave dielectric ceramics, which have high permittivity, are used as materials of microwave components such as resonator, band pass filter and duplexer. These materials received attention due to the rapid progress in microwave telecommunications and satellite broadcasting etc. [3, 4]. The band gap of ZnO can be tuned via divalent substitution on the action to produce heterostructures. Cadmium, (Cd) doping can decrease the band gap to as low as ~ 3.0 eV, whereas Magnesium (Mg) doping can increase the band gap to as high as ~ 4.0 eV. Electron doping in nominally undoped ZnO has been attributed to Zinc interstitials, oxygen vacancies, or hydrogen. With appropriate dopants such as aluminum and galum, it is both transparent in the visible region and electrically conductive [5, 6]. For ZnO, n-type conductivity is relatively easy to realize via excess Zinc or with Aluminum (Al), Gallium (Ga), or Indium (In) doping, but p-type doping has only recently been achieved. This is a fairly common occurrence in wide band gap semiconductors, where difficulty in achieving bipolar "n-type and p-type" doping is not unusual. The most promising dopants for p-type material are the group V elements. Conductivity of ZnO is decreases when heated in oxygen under pressure and when heated in vacuum, its conductivity increases. The change in conductivity of Zinc oxide can also be caused by the addition of varying amounts of monovalent oxides decreases the conductivity whereas addition of trivalent oxides such as Aluminum (Al) or Chromium (Cr) increases the conductivity.

Viorica Musat et al. reported the synthesis of ZnO 1D nanostructures grown on glass substrates seeded with gold layer, pre-prepared ZnO nanoparticles or sol–gel derived ZnO layer [7]. C. W. Cheng et al. observed six fold enhancements in the near band gap emission of ZnO nanorods by employing surface Plasmon of Au nanoparticles, while the defect-related emission is completely suppressed. Time-resolved photoluminescence indicates that the decay process becomes much faster by Au capping [8]. C. W. Lai et al. [9] described that the effects of metal coating on the near-band-edge emission of ZnO thin films have been studied by photoluminescence and atomic force

microscopy. Large enhancement in emission intensity has been observed from ZnO films when they are capped by Ag while negligible effect is seen on Au-coated films. Tatsunori Sakano et al. [10] have been given the description that ZnO nanorods arrays on Si (1 0 0) substrate were grown by the pulsed laser deposition (PLD) method, and then coated with Au. Two samples of Au-coated nanorods arrays with different average diameters of 150 and 400 nm were prepared to investigate the size dependence of the surface enhanced Raman scattering (SERS). Soumen Dhara et al. investigated the mechanism of photo induced charge transport and origin of enhanced PC and PL from Au and Ti NPs decorated vertically aligned ZnO NWs arrays. Uniform decoration of metal NPs on the surface of the ZnO NWs was confirmed by high resolution electron microscopy imaging. Y. G. Wang, et.al reported that Zinc oxide (ZnO) films were synthesized by thermal oxidation of metallic zinc films in air. The influence of annealing temperatures ranging from 320°C to 1000°C on the structural and optical properties of ZnO films is investigated systematically using x-ray diffraction and room temperature photoluminescence (PL) [11]. Zhang et al. reported that single crystalline Fe-doped ZnO nanocantilever arrays have been synthesized by thermal evaporating amorphous Zn-Fe-C-O composite powder.

In this paper, we demonstrated that vertically aligned ZnO nanohairs/ needle could be grown on the Zn metal itself by thermal oxidation methods. The reaction was further catalyzed by the doping of gold in the matrix. This was covered with gold by sputtering technique. Annealing technique was used to introduce the defect in the matrix. In this case, heat treatment was given to the material for 2hr and cooled in the furnace. Surface morphology was investigated from the SEM and phase was characterized from XRD and Raman spectroscopy.The aim of the paper is devoted to examine the influence of annealing behaviour on the structure, morphology and dielectric properties of the ZnO nanostructure material.

Experimental

ZnO nanostructure material was synthesized from thermo-oxidation method. In this case, pure metallic Zn chips (Aldrich, 99.998%) were put inside the silicon crucible which was present at the heating zone. The approximate size of the crucible is around 1.5cm in diameter (cone shape) 2.5cm in depth. The ZnO nanostructures were fabricated in double-walled tubular furnace (Si-rod based system) (see Fig. 1), in which the reaction temperature, carrier-gas flow, and pressure can be independently controlled. The substrates were nearly located at the open end of the small tube, which was put at the heating zone of furnace center. The crucible which contain a Zn –chips was put in the furnace, the furnace heating was switched on and time was recorded after the furnace reached the holding temperature i.e. say 300-700°C. Then the sample was held at that temperature for 2-10 hrs and finally the samples were furnace cooled. Before heating, the chamber was pre-evacuated to a background pressure below 10^{-4} mbar, after which a constant flow of Ar (50 sccm) gas was maintained at a pressure of 200 mbar. Due to a temperature gradient, the temperature around the source was uniformly attained say around ~ 350°C.

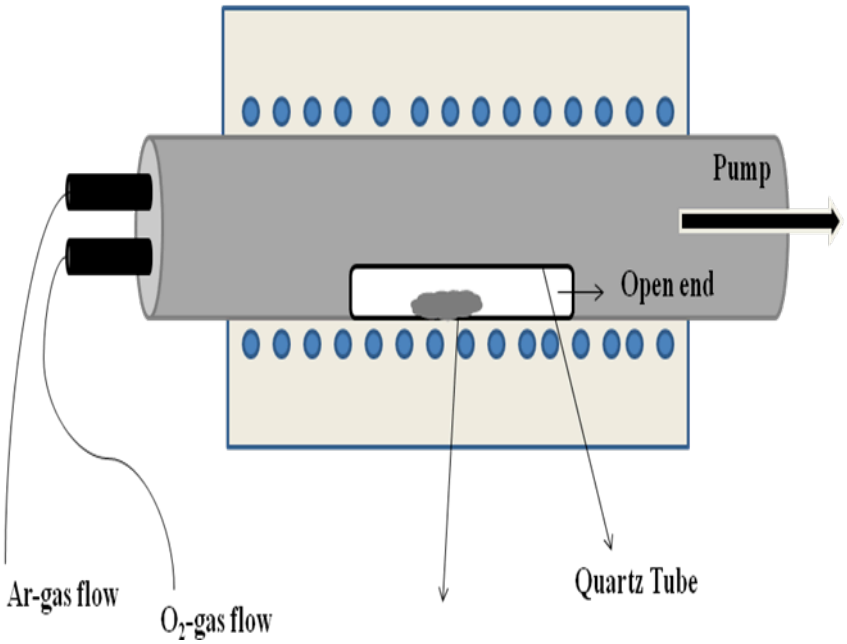

Figure 1 Schematics diagram of the experimental setup and substrate surface after reaction

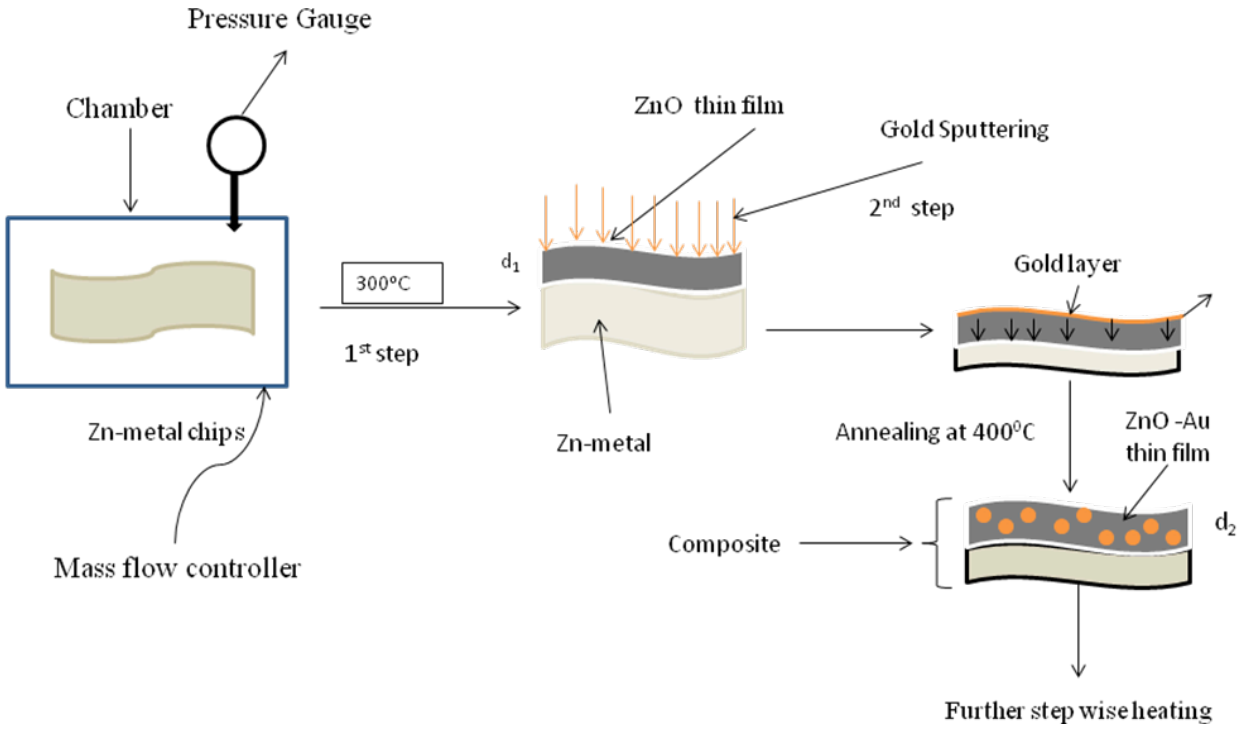

Figure 2 Preparation of ZnO-Au nanocomposite (Schematic view)

When the temperature was raised to 300°C, oxygen was introduced into the system at a flow rate of 4-40 sccm. The flow rate of the gas was controlled by the mass flow controller and the mass flow meter. During growth of ZnO nanorods/needles, the optimized temperatures were held constant for 2-10 h, and then the furnace was switched off and allowed to cool at room temperature. Due to thermal oxidation in the open atmosphere, the chips of the metal after cooling shows drastic change in colour from its initial white to grey indicating the formation of ZnO nanocrystalline at the surface of Zn-metal. Prepared ZnO nanostructure from the above method was covered with Au thin film. From sputtering system (JFC-1600, JEOL auto fine coater), the thin film of gold approximately 2-4 nm size was used to deposit film on the given substrate. In this work, the modified surface of ZnO from the gold was annealed at 400°C for 2-10hr. The coverage of Au nanoparticles was controlled by a current of 20 mA for different sputtering times. Under our system, the deposition rate of the Au nano- film on the substrate is about 0.2 nm s^{-1}.

When the sputtering time is less than about 100s, the deposited Au-film on the ZnO nanorods/nanoneedles is discontinuous, consisting of many nanoclusters, homogeneously dispersed at the surfaces, which were referred to as Au nanoparticles. The size of nanoparticles can be controlled by adjusting the sputtering time. In this preparation, different time intervals were taken to deposit the thin film on the surface. For instance, at a sputtering time of 40 s, the average particle size is about 4–5 nm, and 7–8 nm for a sputtering time of 80 s. The different annealing temperature was selected for the preparation of Au- nanocomposite (see Fig.2).

The crystalline structure and surface morphology of the as-grown product of ZnO nanohairs and their composite were being characterized by scanning electron microscopy (SEM) (JSM 6390A, JEOL) and electron energy dispersion X-ray (EDX). The crystal structures of ZnO nanomaterials were analyzed by X-ray diffraction (XRD) (Diffracto- meter with Cu Ka radiation). The dielectric impedance analyzer was sued to measure the dielectric constant of the composite materials [12].

Results and Discussion

Surface Morphology study

Fig 3 shows SEM micrograph of as received Zn-metal sample used for the experiment under SEM investigation. The surface of the as received Zinc contains 100% Zinc without any traces of Zinc oxide on its surface, investigated through EDAX analysis. The Zn metal is placed at the top position in electrochemical

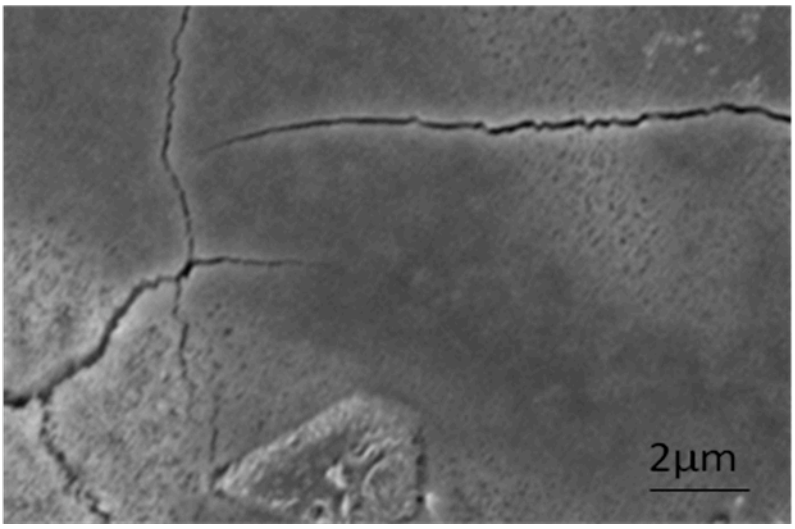

Figure 3 SEM micrograph of Zn-metal (as received)

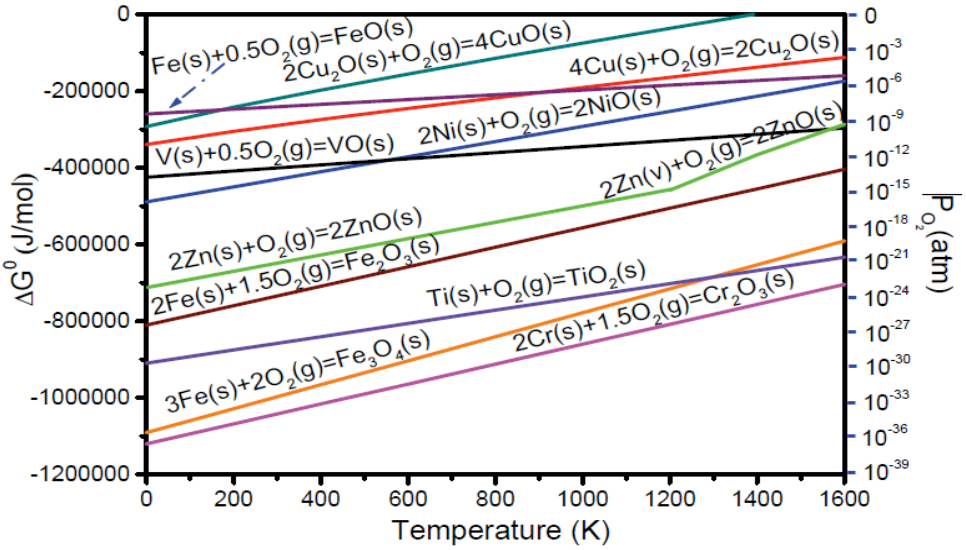

Figure 4 Ellingham diagram

series. They are characterized along with active metal. For long time exposure in open atmosphere, Zn metal easily oxidizes in ZnO from thermal oxidation method. The Ellingham diagram, as shown in Fig 4 is helpful for explaining the formation of stable oxides at the different temperature. The oxygen partial pressure is taken as 1 atmosphere, and all of the reactions are normalized to consume one mole of O_2 [13].

$$2Zn(s) + O_2(g) = 2ZnO(s) \qquad (1)$$

The oxide layer thickening in furnace depends upon the P_{O2} as well as temperature (from Equation (2)). Fig.5 (a) shows the variation of swelling of the oxide layer with the flow of gas. Swelling can be calculated in terms of weight change. The thickness of the layer is measured by Gravimetric method using the electronic balance. According to Gravimetric method, the thickness can be calculated as

$$\text{Thickness} = M/\rho a \qquad (2)$$

Where M is the mass of the deposited film, ρ= density of ZnO and a =area of the film. By using this formula thickness of the growing layer was calculated and it was found that the sizes varies from 60-100µm. It is evident from the Fig.5 that oxide layer is much more thicken at the higher flow rate. Maximum amount of ZnO is

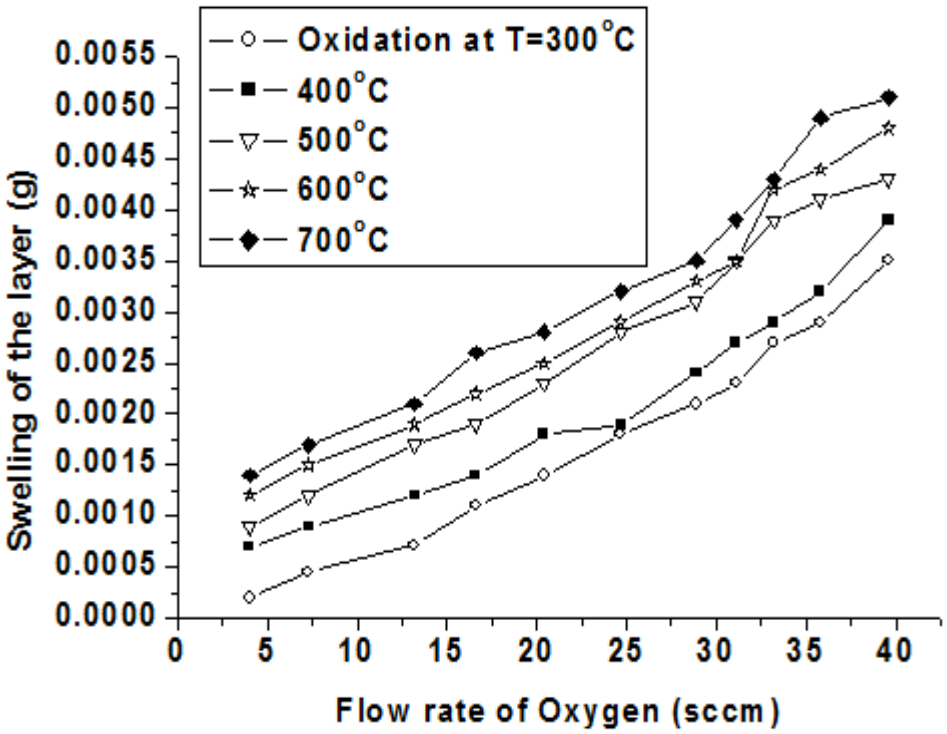

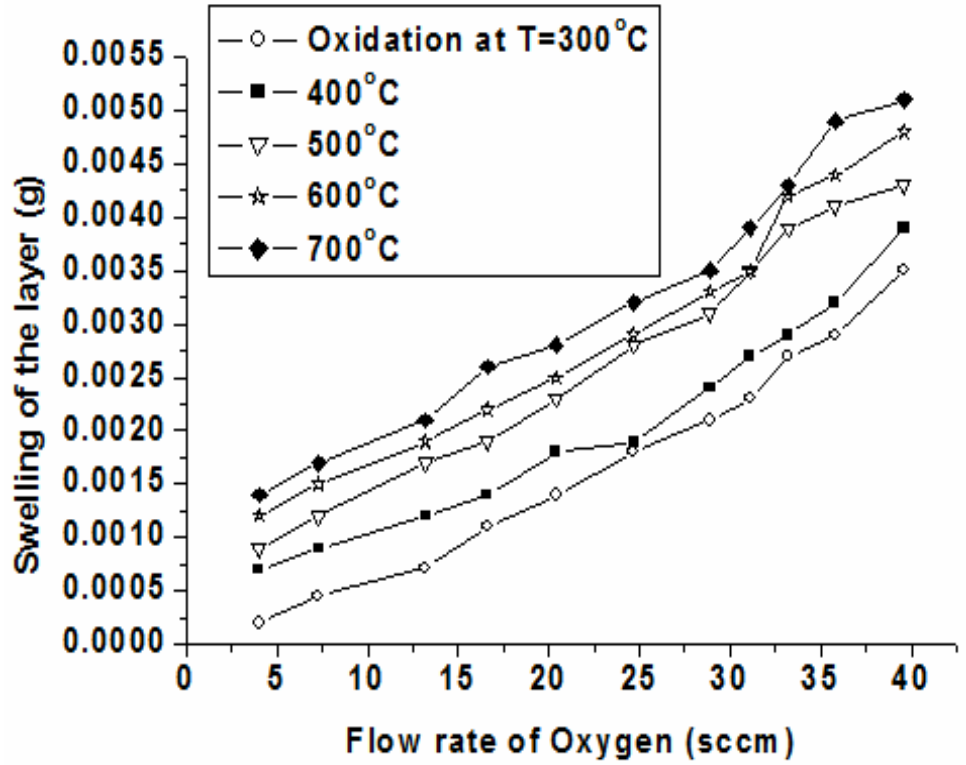

Figure 5 swelling characteristics of ZnO (a) for t different temperature (b) for different time

formed on the surface of zinc. The same trends were obtained at the higher temperature. Fig.5 (b) shows the swelling characteristics of ZnO with respect to time. In this case, the flow rate of oxygen was kept constant. In maximum time, swelling characteristics of ZnO layer is found maximum. It is also evident from the Fig 5(b) that the swelling of the ZnO layer increases with increase the flowing time of Oxygen.

The SEM morphology of oxidised layer of ZnO at 300^{o}C is shown in Fig.6 (a). It is clearly seen in figure that the needle type of the oxide layer starts to grow at the surface. The clarity in the image was obtained at the higher magnification in Fig.6(c). The formation of ZnO was again confirmed by EDAX analysis, as shown in Fig.6 (d)**.** This analysis was easily predicting the existence of ZnO at the mative surface. Fig.6 (b) shows the Raman spectra of the ZnO nano crystalline material. Space group of hexagonal wurzite ZnO belongs to C^{4}_{6v} with two formula units per primitive cell. According to group theory, single crystal ZnO has eight sets of optical phonon modes at G point of brillouin zone classified as $A_1 + E_1 + 2E_2$ modes (Raman active), $2B_1$ modes (Raman silent), and $A_1 + E_1$ modes (infrared-active). Moreover, the A_1 and E_1 modes split into longitudinal (LO) and transverse optical (TO) components.

Fig. 6(b) shows that a Raman spectrum of ZnO nano needle exhibits only E_2 modes at 438± 2cm^{-1}. In this measurement, Raman spectrum was recorded in the backscattering geometry mode with incident light exactly perpendicular to the surface of ZnO nano-needle, viz. incident light parallel to the axis of ZnO nano-needle.

In this configuration, only E_2 and A_1 (LO) modes are allowed and infrared active, and meanwhile the A_1 (TO) and E_1 (TO) modes are forbidden according to the Raman selection rules. This is out of region from the spectrum. The absence of TO modes in Raman spectra could be attributed to special angle between the wave vectors of photons and c axis direction of wurzite ZnO crystals. The c-axis wurzite ZnO crystal is out of interaction with the axis of Laser light only ab-plane interacts with the light.

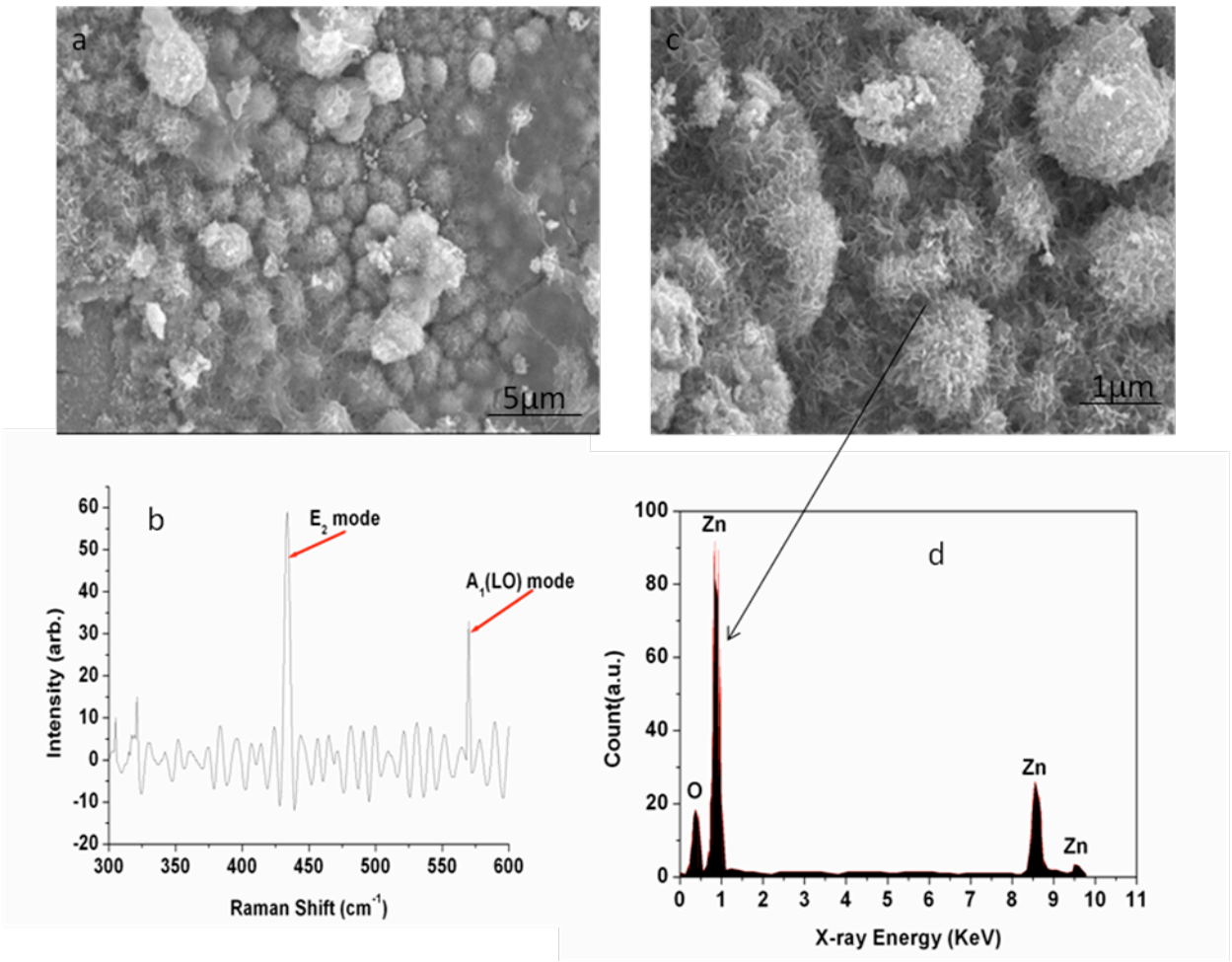

Figure 6 SEM images of ZnO nanoneedle grown on Zn-metal surface. (a) Low magnification image well-aligned ZnO nanoneedle. (b) Raman spectra of ZnO nano film. (c) The magnified image of ZnO nano-needle from an oblique view angle (d) EDAX analysis of the film.

Fig.7 illustrated the XRD pattern of ZnO nanocrystals prepared by thermal oxidation methods. The diffraction peaks of sample were quite similar to those of bulk ZnO, which can be indexed as the hexagonal wurtzite structure ZnO and diffraction data were in agreement with JCPDS card of ZnO (JCPDS card No. 36-1451). No peaks other than ZnO were detected. The main peak appears at 2θ=36.71. Thus the results obtained from thermal oxidation of Zn metal showed that only single phase hexagonal ZnO can be obtained on the surface. We can evaluate the mean grain sizes (GS) of the thin films using Scherer's formula:

$$D = \frac{0.9\lambda}{B\cos\theta} \qquad (3)$$

Where D is the crystallite size, k is a constant (= 0.89 assuming that the particles are spherical), λ is the wavelength of the X-ray radiation, β is the line width (obtained after correction for the instrumental broading), and θ is the angle of diffraction. The average size obtained from the XRD data is 34 nm. Meanwhile, some weak peaks at 2θ= 31.91, 34.61, 47.61 and 63.21 also appear on the spectra of some films, which can be attributed to (1 0 0), (0 0 2), (1 0 2) and (1 0 3) diffraction peaks of the hexagonal ZnO, respectively.

As the oxidation temperature increases from 300 to 700°C, all of the thin films show a main peak at 2θ =36.71, which corresponds to the (1 0 1) diffraction peak of the hexagonal ZnO. The intensities of (1 0 1) peaks increase and reach a maximum at 500°C, and then decrease. By taking into account that the melting point of metallic Zn is 419.5°C, when the oxidizing temperatures are much higher than the melting point, the Zn metal under the thin films of top ZnO layers will melt, resulting in the supplement of oxygen to the Zn layers and the limitation of the continuous growth of the oxide grains. Therefore better results are obtained at the elevated oxidation temperature and the length of oxidation duration. The thin films consist in this case of polycrystalline grains with no preferential orientation of growth. The average sizes of crystallites are about 70.5 nm (for the films annealed at 300 °C) and 97.2 nm (at 700 °C). Increasing the annealing temperature makes the diffraction peaks better pronounced and increases the size of crystallites.

Increasing the annealing temperature causes a transition from orthogonal in to hexagonal structure, respectively from Zn $(OH)_2$ toward ZnO. The (100), (002), (101) diffraction peaks of ZnO films appear clearly at a higher annealing temperature, which can be indexed as the hexagonal wurtzite structure of ZnO. All the peaks attributed to the metallic Zn disappear when the oxidation temperature reaches 600°C, which indicates that the metallic Zn was transformed to ZnO completely at this temperature. Thus, the grain sizes increase with increasing oxidation temperatures. The relationship between annealing temperatures and the corresponding ZnO crystallite sizes are summarized and as illustrated in Fig. 8, respectively.

Fig.9 shows the schematic view of gold diffusion inside the ZnO thin film through annealing processes. By repeating processes, gold homogenously scatter in the ZnO thin film. This forms immiscible alloy with each other. They provide the nucleating sites for growing the ZnO needle like structure on the zinc surface. The metal-oxide nuclei arrangement was designed based on the nuclei probability in term of the minimization of surface energy. As discuss above, a nucleation will form when it can overcome the maximum energy barrier, ΔG_N^*.Thus, we can write the probability of nucleation, P_N, and given

$$P_N = \frac{N}{N_o} = \exp(-\Delta G_N^* / k_B T) \qquad (4)$$

Where N is the surface concentration of nuclei and N_0 is the possible surface concentration of nuclei on metal surface, k_B is Boltzmann constant and T is temperature. It can be seen that the magnitude of P_N depends on three parameters; temperature, surface energy, and ΔG_N^*. Fig.10 shows the PB ratio of oxide formation at the metallic surface. With the passage of time, maximum amount of metal-zinc converts into ZnO nano-needle. This reaction was further catalysed by the presence of Au inside the film as shown in Fig.8. In this case, double amount of ZnO- nano-needle are formed, i.e., $(PB)_f \approx 2 (PB)_i$ whereas $(PB)_f$ is the Pilling-Bedworth ratio in presence of gold and $(PB)_i$ without catalyst. That means the reaction kinetics was catalyzed nearly two times in presence of gold. Besides the Au, this reaction also depends upon the flow rate of oxygen within the reacting box.

At the partial pressure of oxygen inside the reacting the box, the oxygen diffuse very fast inside the film, and activate the gold particles for catalyze the nucleation. At the higher temperature, maximum amount of gold diffuse inside the film, and alter the kinetic of the reaction. These results were again checked from swelling measurement of ZnO thin layer in presence of Au at different temperature with flow time of oxygen in reaction chamber. Their beautiful results were presented in Fig.11. The swelling of ZnO layer increases with flow time but argument is valid for temperature. Time and temperature helps the growing of oxide layer on the Zn-metal surface. The result was investigated through SEM and presented in Fig.11 a to e. Heating of Au-coated surface, hairs like needle structure of ZnO were grown very fast at the surface, as shown in Fig.11 (a). But at the higher magnification, hairs like structure of ZnO, approximately one tenth of micrometer is clearly visible as shown in Fig 11(b). Maximum hair of ZnO was nucleated at the 700°C as shown in Fig.11 (f). It should

be noted that al thought ΔG^*_N for heterogeneous nucleation have a function of shape factor, the characteristic curve is not different, compared with the spherical homogeneous nucleation.

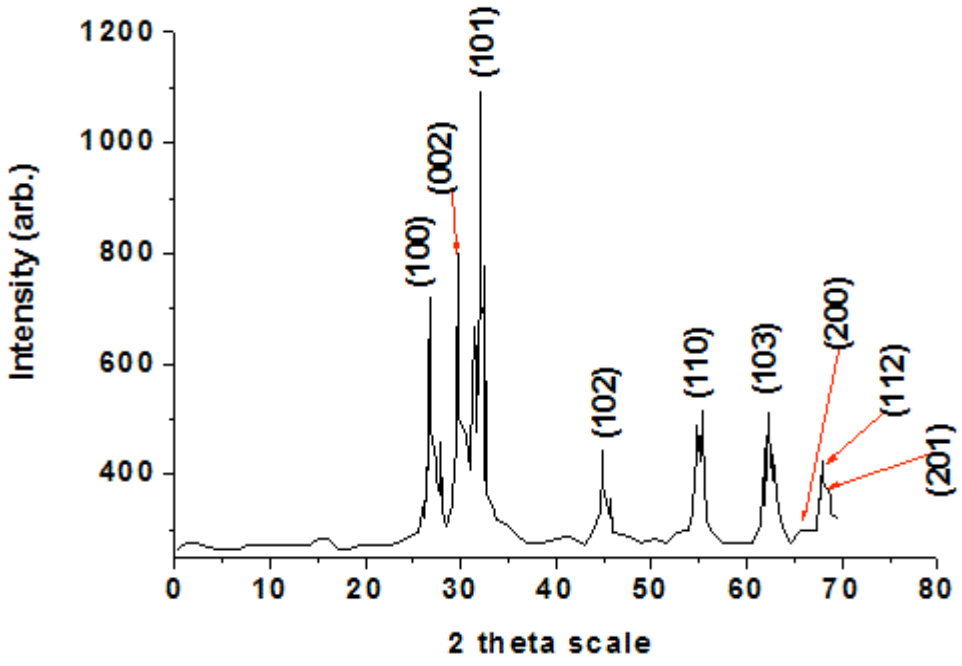

Figure 7 XRD pattern of pure ZnO formed on Zn-metal surface at 400°C

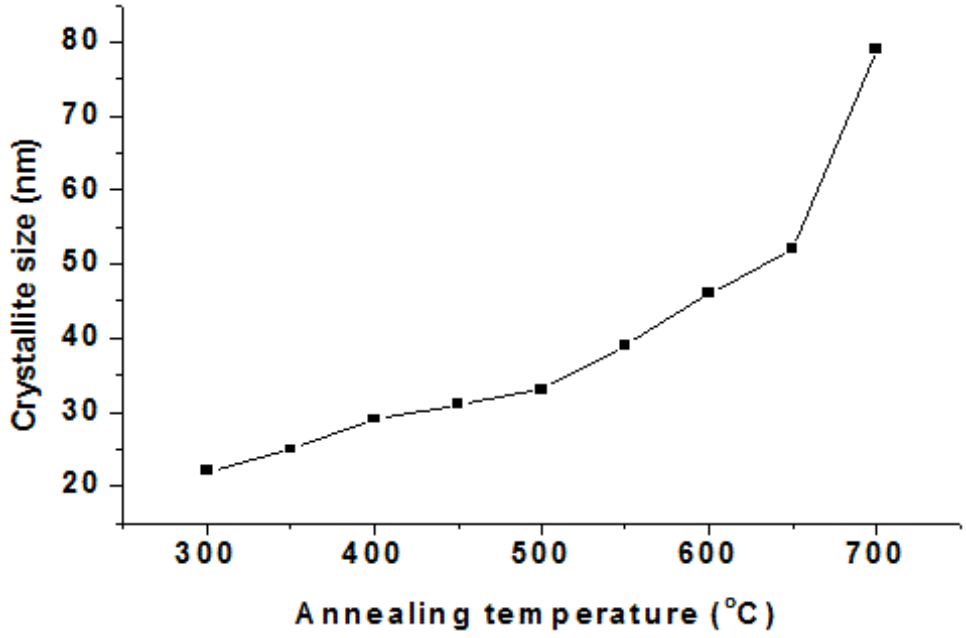

Figure 8 Relationship between the crystallite size of ZnO and the annealing temperature

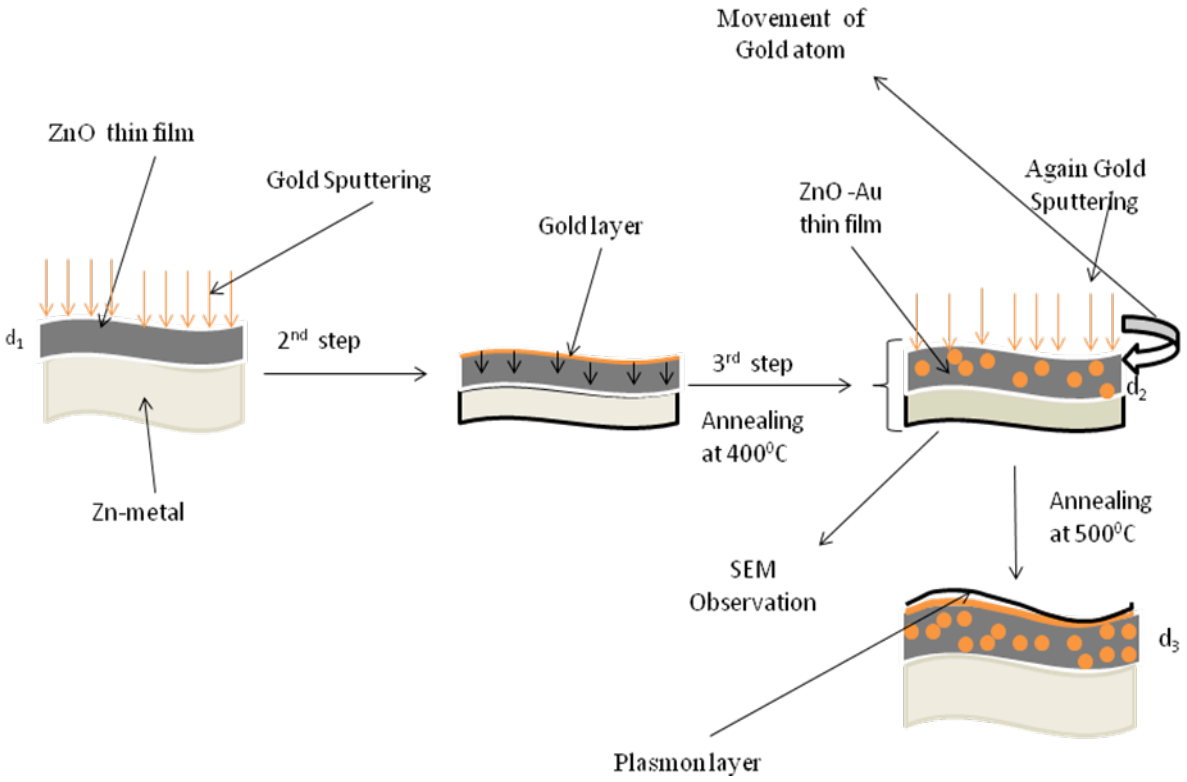

Figure 9 Schematic diagram of Au-atom diffusion inside the ZnO film

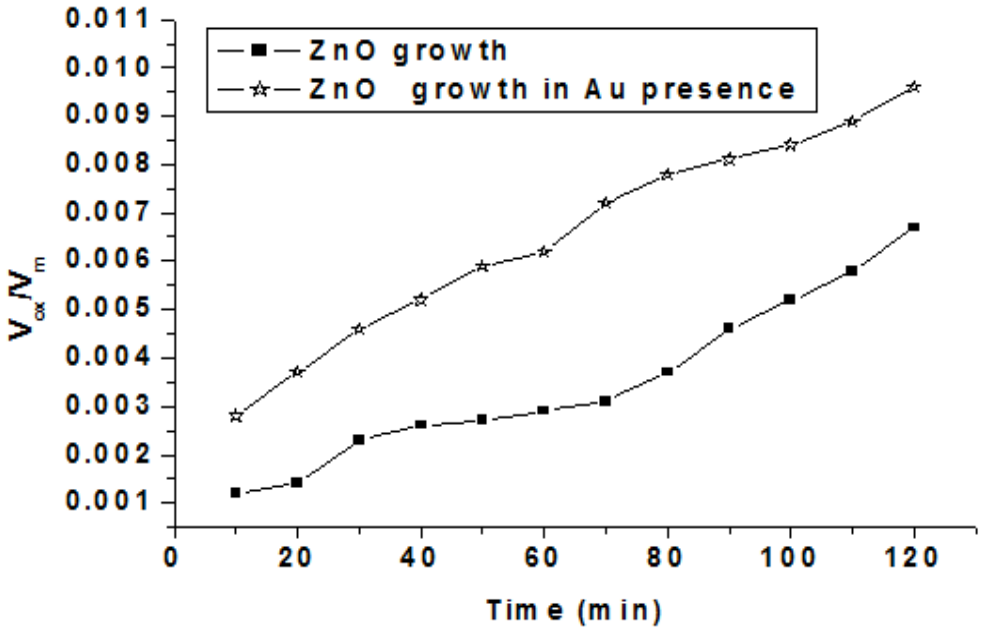

Figure 10 PB ratio of growth of ZnO nano-needle structure with and without the presence of Au at the 300°C.

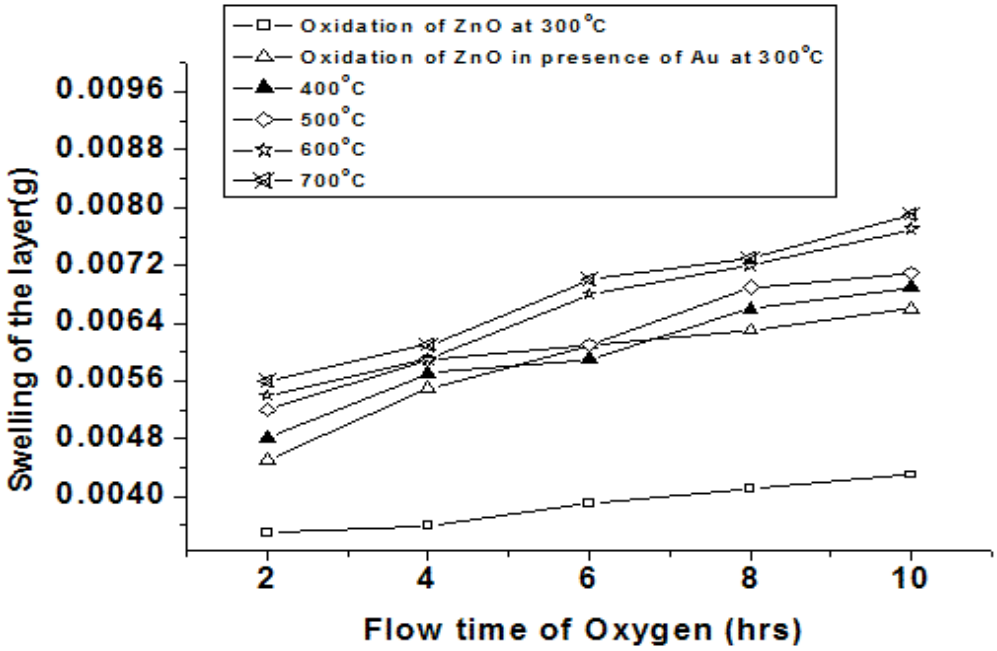

Figure 11 Swelling characteristics of ZnO-Au nano-composite with flow time of oxygen

The shape factor just describes the magnitude of the decreasing energy barrier ΔG^*_N. Necking which was analysed through the EDAX analysis, along with XRD investigation. When the sample were annealed for two hours, the Zn-foil showed some reduction in size and with EDAX studies confirm the presence of ZnO as the ratio of Zn and O (21.33 at % and 25.31 at % O) and rest along with Au as shown in Fig.12.(a). In Fig.12 (b) different peaks of ZnO at the different angle along with Au are seen in the monograph. Due to annealing, Au only diffuses in the lattice and doesn't react with ZnO film. In this case, Zn metal act as surface at which ZnO layer starts to grow and their peak are found at the higher scanning angle. The XRD pattern of ZnO nanowires reveals a wurtzite structure for the nanowires. The lattice constants of ZnO nanowires are a = b = 3.26 Å and c = 5.22 Å. No other diffraction peaks, such as Zn, Au, are detected in our samples. The particles were in the order of nano range approximately 35-40nm, i.e., ZnO nano hairs like structure of equal size can be seen on the surface of metal, as presented in Fig. 11 (c), but they were seen elongated form at the higher magnification as seen in Fig.11 (d).

Due to catalytic activity of gold and enhanced action of reaction at 400°C, many more hair spots were quickly formed on the surface of metal, as compared to 300°C. Subsequent sputtering and annealing at 700°C for 2hr in open atmosphere, the obtained spots of ZnO nano crystalline structure along with Au were again confirmed with EDAX analysis and their results shows that at. % of Zn (31.37 %) and O (33.43%) and rest of Au are almost identical suggesting that highly stoichiometric ZnO is formed at this temperature. The SEM observation of the growing film on the surface shows that rod like or needle like structure of ZnO whose thickness reduced optimum height and minimum tip diameter are formed at temperature 700°C, as shown in Fig.11(e) & (f). From the above investigation of the systematic results on the bias of obtained data, the proposed mechanistic approach of the growing ZnO nano-needle in the presence of Au nano-particle at the self-initiating surface is shown in Fig.13. In this case Au atom starts to diffuse inside the film but they are not retained their. The explanation is based on the basis of crystal structure of the considered material. ZnO exhibits wurtize structure and Au fcc structure. But their alloy is not possible. Therefore ZnO try to push the Au from inside to outside because of continuous diffusion of O_2 from the outside source. The ZnO film is continuously grown on the surface from the inward to out ward due to adsorption of O_2 molecules. Baubles are formed at the surface. Due to fast cooling from the surface by convention and conduction processes, the bubbles are tried to convert into tip form, as shown in Fig.13. It is observed through the SEM investigation, the ZnO nano-needle have a length of 35-40 nm and diameter of 2-4nm. Clearly, the bare ZnO nano-needle oriented in certain direction has a smooth surface, while for the Au/ZnO after repeating sputtering and step wise annealing, Au nano-particles with diameters of about 5 nm are uniformly distributed on the surface of the ZnO needle confirmed through EDAX analysis. Reasonably, the sizes and the diameter of the Au particles at the ZnO nano-tips for Au/ZnO with 20 and 100 s sputtering time are respectively smaller and larger than 5 nm.

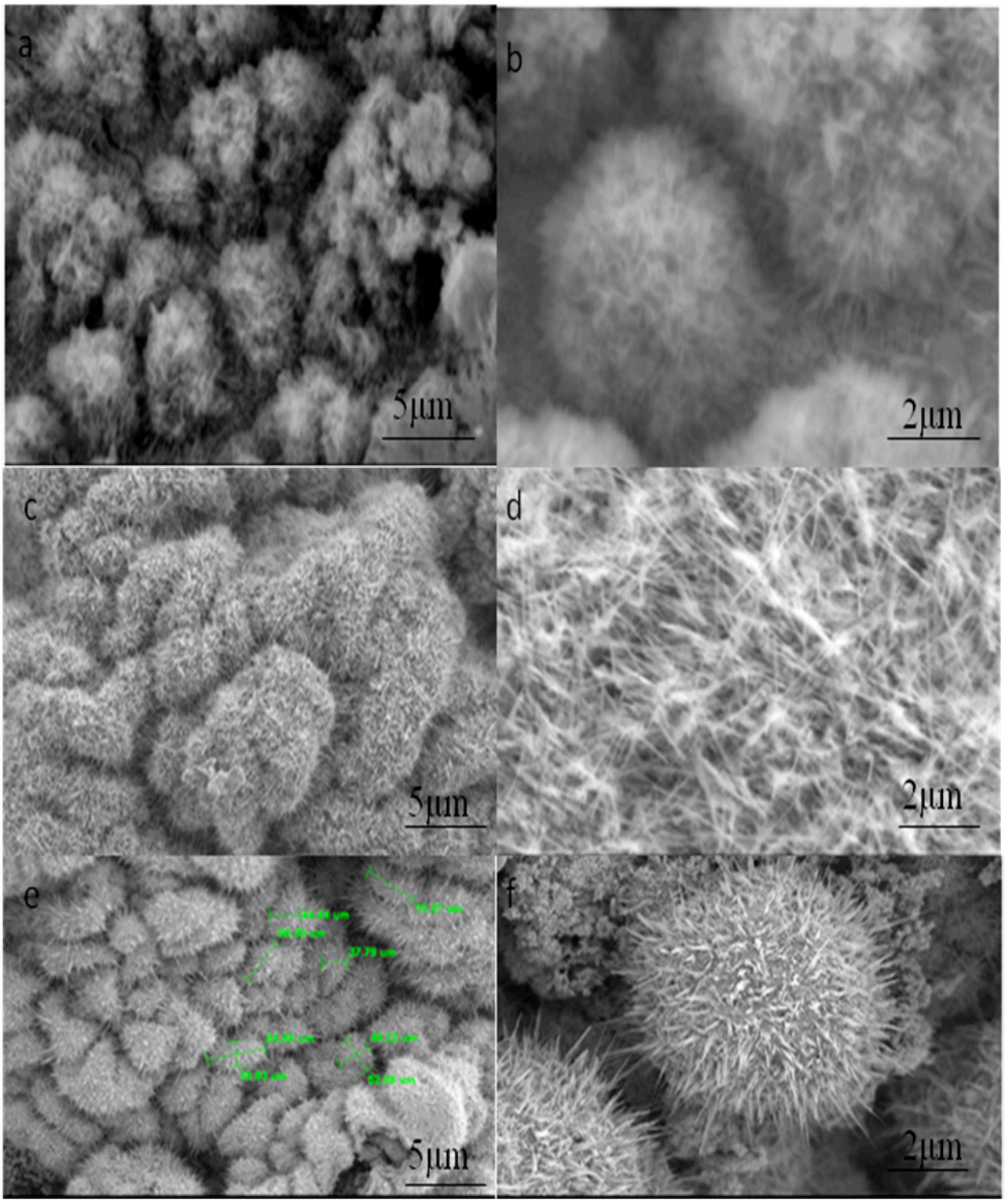

Figure 11 SEM morphology of ZnO nano-needle (a) & (b) at 400°C, (c) & (d) at 500°C (e) and (f) at 700°C

Dielectric Measurements

$$C = \frac{\kappa \varepsilon_o A}{d} \qquad (5)$$

The capacitance performance can be calculated using above equation (1)

Where C is the capacitance, ε_0 is permittivity of vacuum, ε_r is relative permittivity also known as dielectric constant, A is the area of electrode and d is the thickness

of the dielectric layer. From the formula, it shows that the relative permittivity (dielectric constant, *k*) and also dielectric thickness are the important parameters that will influence capacitor performance.

$$\varepsilon_r = \frac{t \times C}{A \times \varepsilon_o} = \frac{t \times C}{\pi(\frac{d}{2})^2 \times \varepsilon_o} \qquad (6)$$

Where,

t =Thickness of the pellet

C= Equivalent parallel capacitance which obtained from the data of measurement

ε_0 =permittivity of vacuum = 8.854 x 10^{-12} (F/m)

d = Diameter of guard electrode = 5 x 10^{-3} (m)

Thus, the above equation becomes,

$$\varepsilon_r = \frac{t \times C}{6.25 \times 10^{-6} \times \pi \times \varepsilon_o} = \frac{t \times C}{1.74 \times 10^{-16}} \qquad (7)$$

Whereas, the imaginary permittivity or dielectric loss, ε_i , is obtain from the value of dissipation factor, *D*. Where, dissipation factor, *D*,

$$D = \frac{\varepsilon_i}{\varepsilon_r} \quad , \quad \varepsilon_i = D\varepsilon_r \qquad (8)$$

The relative permittivity ε_r of the nano crystalline material measured at room temperature versus frequency of the applied LCR meter ranging from 1 kHz to 5 MHz with annealing temperature as the function is shown in Fig.14. This data was taken when the ZnO was trying to develop at the Zn metal surface. The synthesis of ZnO depends upon the partial pressure of the oxygen gas inside the furnace. The dielectric constant of the material was found to be decrease with increase the operating frequency. For the sample annealed at 700°C, the ε value decreased from 89.1 at 1 Hz to 25.2 at 1 kHz and to 18.4at 1 MHz. The dielectric constant shows the increase tendency with increasing the sintering temperature from 300°C to 700°C. The composite material was developed by the reinforcement of Au within ZnO matrix. This is possible by sputtering technique with subsequent annealing at the different temperature. Fig. 15 represents the variation of dielectric constant measured at room temperature for different frequency as a function of the sintering temperature. The obtained results from the dielectric measurement of the composite material along with pure ZnO was compared and found that the composite material shows higher dielectric constant. By the distribution of gold inside the matrix at the different annealing temperature, the dielectric constant of the nano material increased from 89.1 to 105.6 at 1Hz.

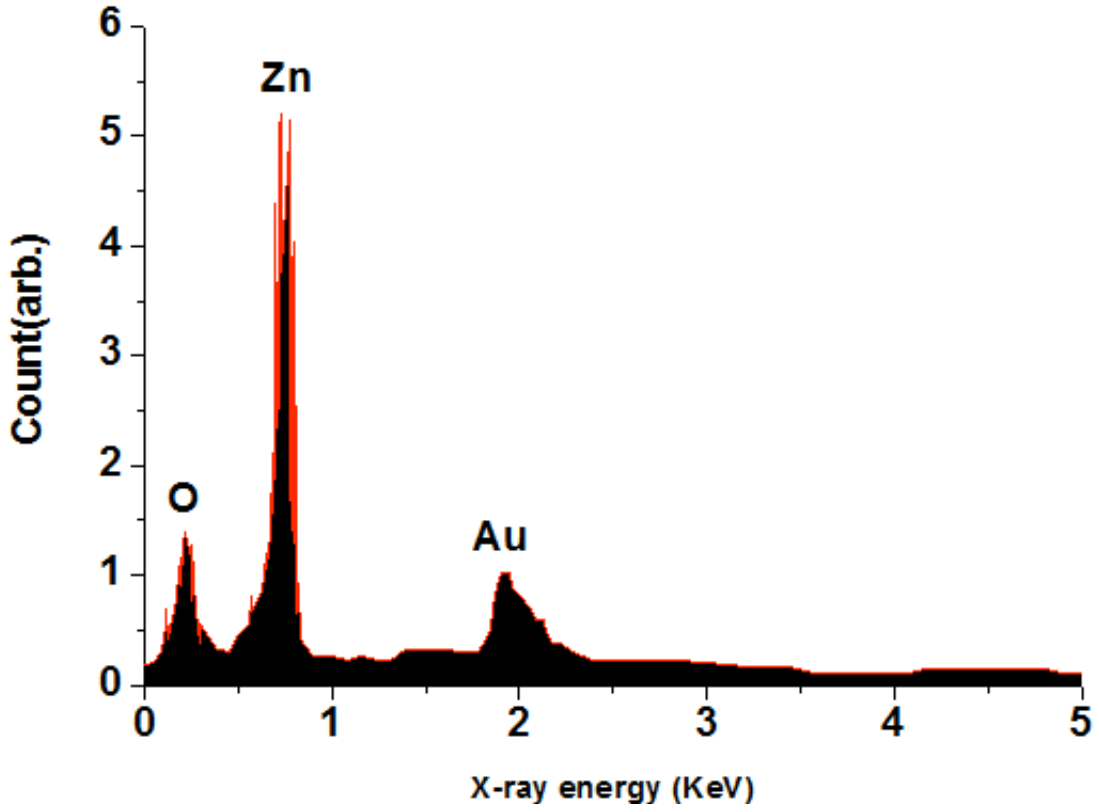

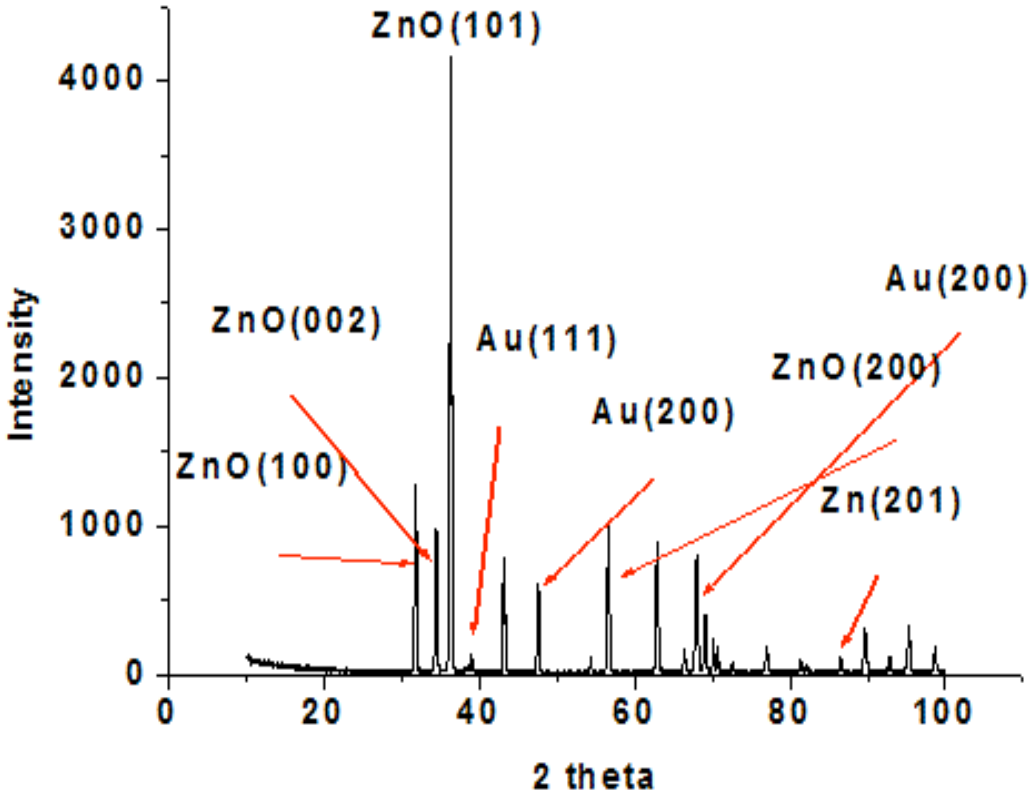

Figure12 (a) EDAX of ZnO-Au nanocomposite (b) XRD of ZnO-Au nanocomposite

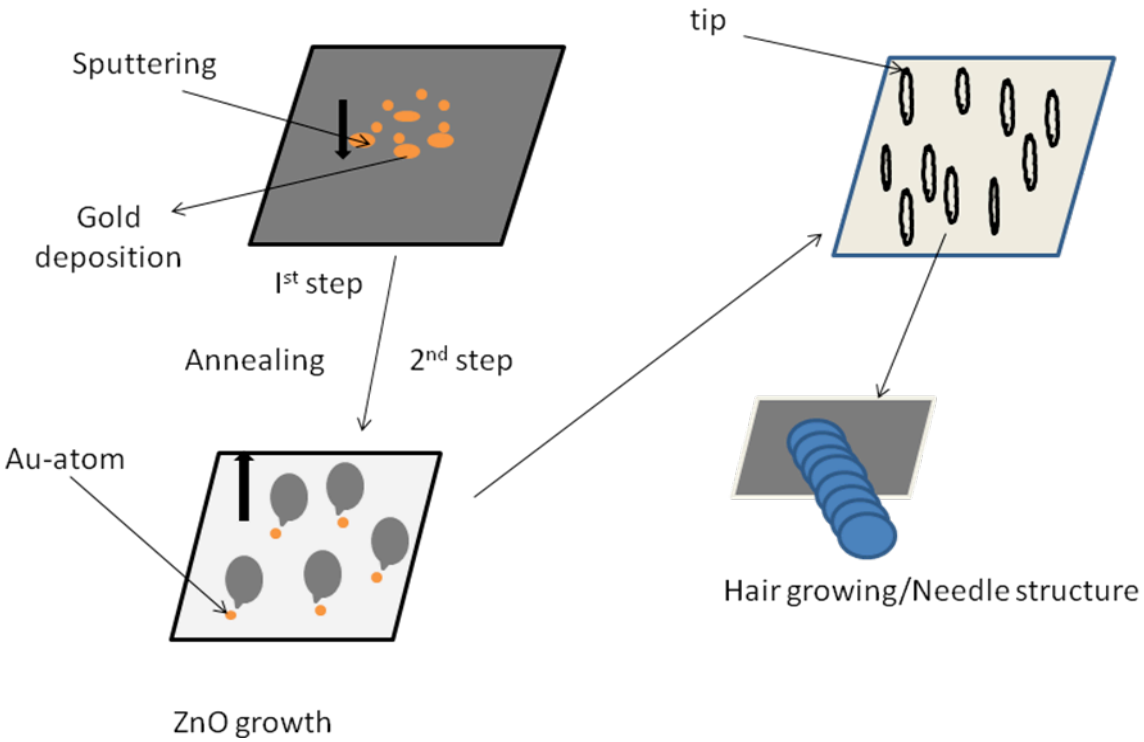

Figure 13 Schematic diagram of Au-atom diffusion inside the ZnO film

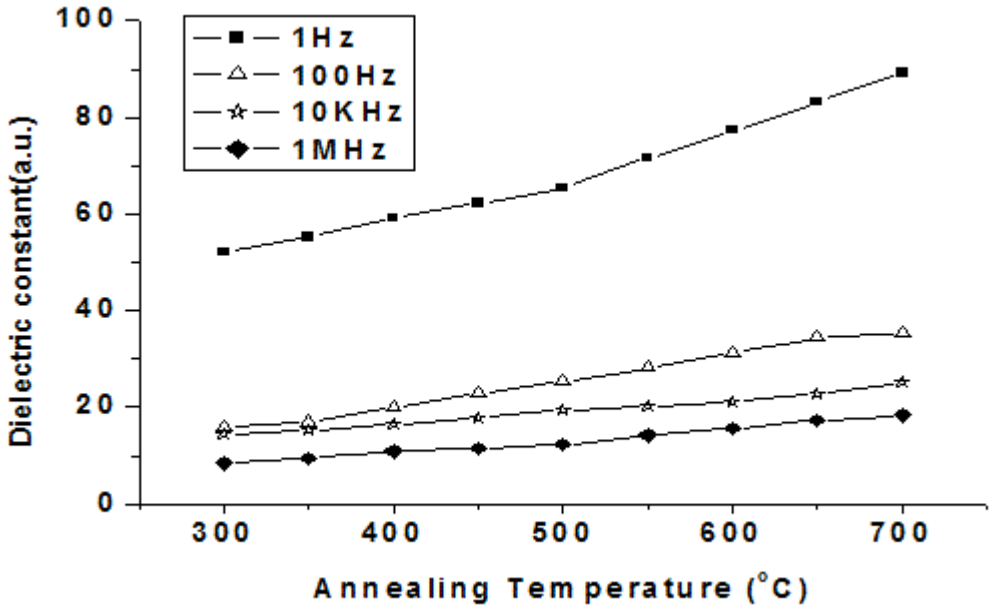

Figure 14 Variation of the dielectric constant as a function of the annealing temperature of ZnO Nano crystalline material

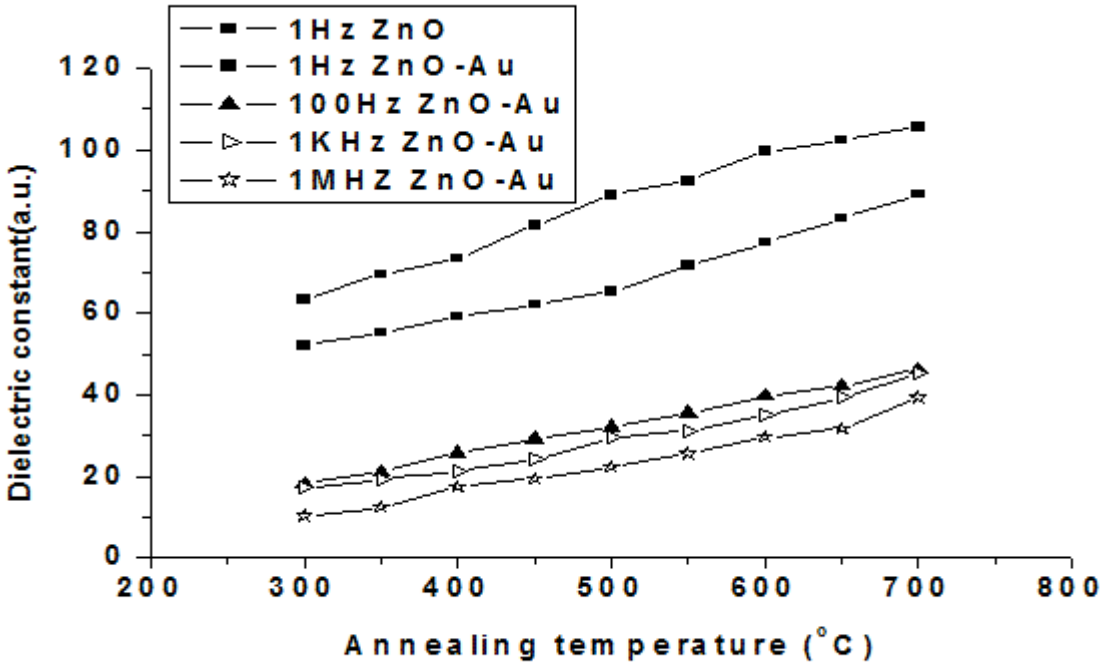

Figure 15 Variation of the dielectric constant as a function of the annealing temperature of ZnO-Au Nano crystalline material

This enhancement was obtained each and every applied frequency. The dielectric constant increases linearly with annealing temperature, was maintained in both the figure, i.e., Fig 14 &15. The imaginary part of permittivity or dielectric loss εi versus frequency of the applied field ranging from 100Hz to 1MHz with the temperature as the function is shown in "Fig 16". As shown in Fig. 16, the lowest value of dielectric loss at higher frequencies ($\tan \delta = 6.23 \times 10^{-2}$) is found for the ZnO nano needle sample annealed at 550°C.The pellet's dielectric loss, ε_i are decreasing with increasing frequency. ZnO nano structure that were developed at 300-700ºC, have large dielectric loss comparable to εi of sintered pellet at 550ºC. This indicates that they can store more energy due to small loss. Hence, they possess dielectric behavior. Meanwhile, εi for annealed at the other temperature is high, indicates there are increasing of dielectric loss. Thus, it cannot store energy, therefore it possess conductor behavior. The same result was found in ZnO-Au nanocomposite. Their optimum value also shows at 550°C, as shown in Fig.17. To compare the Fig.16 with 17, the dielectric loss is found to be minimum ($\tan \delta = 4.12 \times 10^{-2}$) in ZnO-Au nanocomposite at each frequency. But the trends are almost the same.

Conclusion

The following conculsion were drawn on the basis of chosen study:

1. Nano needle or nanohair of ZnO was sucussfully prepared from thermal oxidation methods. The growing of nanohair depndes on controlling the oxygenpartial pressure.
2. PB ratio increase with increase the time of flowing oxygen gas. Growth of nanowire occurs by the continouly adsorbed the oxygen gas on the surface.
3. Swelling charcteristics also depneds upon flowing rate of the gas. Maximum swelling is found at the maximum flow rate.
4. Reaction was also studied in persence of gold. Gold enhance the thickness of ZnO layer. The surface modification of ZnO film is possible by introducing the gold atom in the lattice. They are characterized through SEM analysis.
5. Maximum amount of the hair are grown on the surafce in presence of gold.
6. The SEM results explain the possible mechanistic approaches of the Nano hair growth. The chemical composition at each point during investigation was determined by EDX analysis and the results predicts the possible compsition of element at analysed area.
7. The temperature dependence dielectric constant were studied at room temperature for different frequencies ranging from 10 Hz to 10 MHz. Results show an increase of dielectric constants with increasing the annealing temperature and a decrease with changing the measuring frequency.

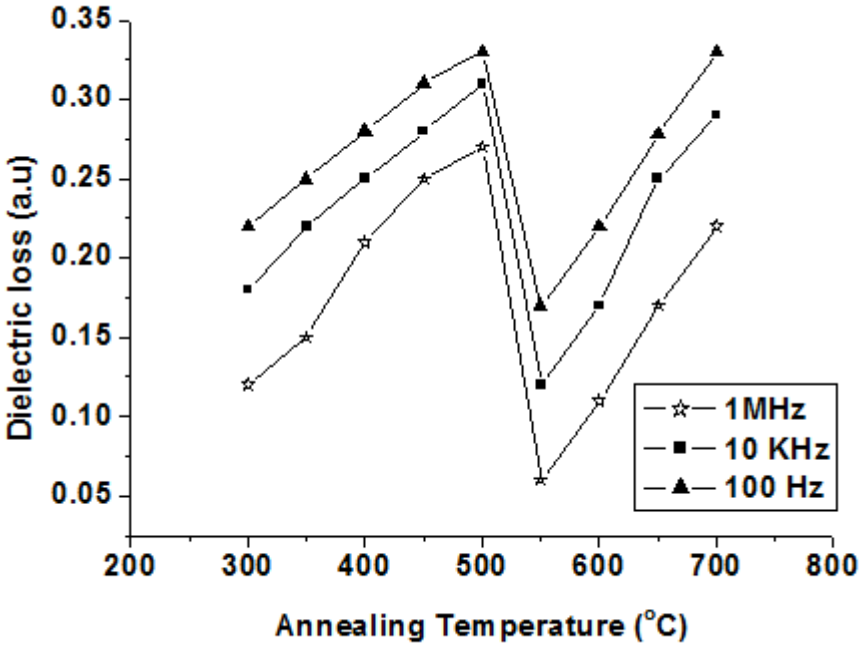

Figure 16 Variation of the dielectric loss as a function of the annealing temperature of ZnO Nano crystalline material

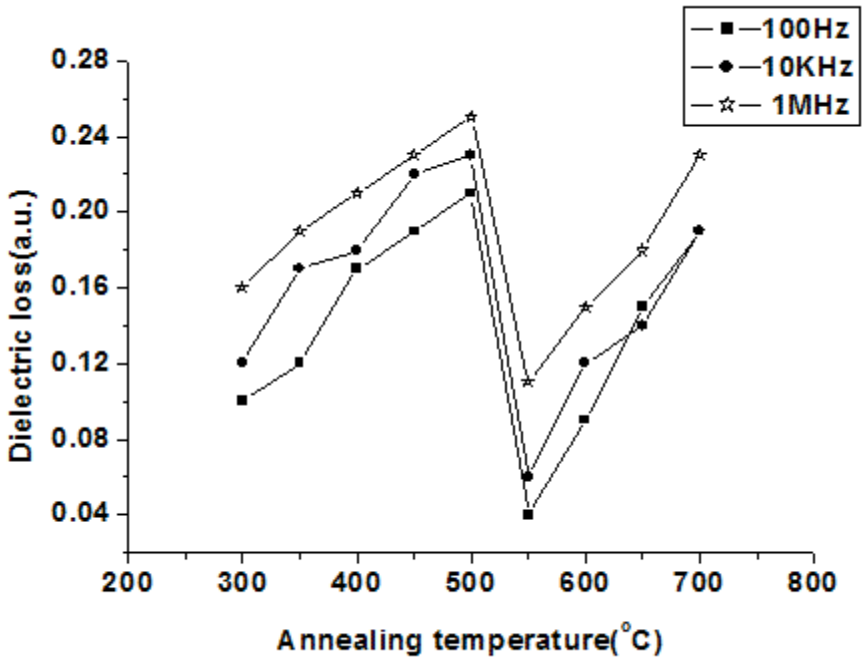

Figure 17 Variation of the dielectric loss as a function of the annealing temperature of ZnO-Au Nano crystalline material

References

[1] Z. K. Mohamad, H. Mamat, M.M. Zahidi, M. Rusop, Japanese Journal of Applied Physic, **2011**, vol. 50.

[2] K. B. K. P. Raji, Recent Research in Science and Technology, **2011**, vol. 3.

[3] Ji-Won Choi, Jong-YOON HA, Chong-Yun KANG, Seok-Jin YOON, Hyun- Jai KIM, Ko Hyun Yoon, Jpn. *J. Appl. Phys*. **2000**, 39, 5923.

[4] C.E. Holcombe, N. L. Dykes, *J. Am. Ceram. Soc*. **1991**, 21, 375

[5] B. N. Mbenkum, N. ashkenov, M. Schubert, M. Lorenz, H. Hochmuth, D.Michel, M. Grundmann, *J. Appl. Phys. Letters.* **2005**, p86 , 091904-1.

[6] S. K. Nandi, S. Chatterjee, S. K. Samanta, G. K. Dalapati, P. K. Bose, S. Varma, S. Patil, C. K. Maiti, *Bull. Mater. Sci*. **2003**, 26, (4), 365.

[7] V. Musat, E. Fortunato, M. Purica, M. Mazilu, A. M. B. Rego, B. Diaconu, Tito Busani, Materials Chemistry and Physics, **2012**, Volume 132, Issues 2–3, Pages 339–346, 15 February

[8] C. W. Cheng, E. J. Sie, B. Liu, C. H. A. Huan, T. C. Sum, H. D. Sun, H. J. Fan , Appl. Phys. Lett. **2010**, 96, 071107.

[9] C. W. Lai, J. An, H. C. Ong, Appl. Phys. Lett. **2005**, 86, 251105,

[10] M. Terakawa, Y. Tanaka, Go Obara, T. Sakano, M. Obara, Applied Physics A: Materials Science & Processing, **2011**. Volume 102, Number 3, 661-665.

[11] T. Sakano, Y. Tanaka, R. Nishimura, N. N. Nedyalkov, P. A. Atanasov, T. Saiki, M. Obara, Journal of Physics D, **2008**.Applied Physics Volume 41,

[12] Y. G. Wang, S. P. Lau, H. W. Lee, S. F. Yu, B. K. Tay, X. H. Zhang, H. H. Hng, J. Appl. Phys. **2003**, 94, 354.

[13] A. J. Shukla, M.Tech Thesis, Surface Modification of ZnO Nanostructure Coated with the Fe (II) / Fe (III), **2012**, School of Engineering, Sharda University Greater Noida, India.

Received : 01st July, 2012
Revised : 05th August, 2012
Accepted : 07th August, 2012
Online : 27th September, 2012